

8-2017

# Peptide-directed Nanoparticle Synthesis With A Denovo Pd-binding Sequence Fused To A Reporter Protein

Rita Eloisa Tejada Vaprio  
*University of Arkansas, Fayetteville*

Follow this and additional works at: <http://scholarworks.uark.edu/etd>

 Part of the [Nanoscience and Nanotechnology Commons](#), and the [Other Chemical Engineering Commons](#)

---

## Recommended Citation

Tejada Vaprio, Rita Eloisa, "Peptide-directed Nanoparticle Synthesis With A Denovo Pd-binding Sequence Fused To A Reporter Protein" (2017). *Theses and Dissertations*. 2393.  
<http://scholarworks.uark.edu/etd/2393>

This Thesis is brought to you for free and open access by ScholarWorks@UARK. It has been accepted for inclusion in Theses and Dissertations by an authorized administrator of ScholarWorks@UARK. For more information, please contact [scholar@uark.edu](mailto:scholar@uark.edu), [ccmiddle@uark.edu](mailto:ccmiddle@uark.edu).

Peptide-directed Nanoparticle Synthesis With A Denovo Pd-binding  
Sequence Fused To A Reporter Protein

A thesis submitted in partial fulfillment  
of the requirements for the degree of  
Master of Science in Chemical Engineering

by

Rita Tejada Vaprio  
University of Arkansas  
Bachelor of Science in Chemical Engineering, 2015

August 2017  
University of Arkansas

This thesis is approved for recommendation to the Graduate Council.

---

Dr. Robert Beitle  
Thesis Director

---

Dr. Roger Koeppe  
Committee Member

---

Dr. Nicholas Bedford  
Committee Member

---

Dr. Lauren Greenlee  
Committee Member

## **Abstract**

There is a need for low-cost nanoparticle materials in the context of new technologies for catalyst development. The purpose of this work was to recombinantly produce a 45- amino acid long metal binding peptide that is useful for nanoparticle synthesis. Using splicing by overlap extension PCR, a synthetic gene containing the fusion of the metal binding peptide with Green Fluorescent Protein (GFP<sub>UV</sub>) was constructed. The metal binding peptide, fused to reporter protein GFP<sub>UV</sub>, was expressed using high cell density fermentation. Palladium nanoparticles of an average diameter of  $1.18 \pm 0.45$  nm were synthesized by using the crude cell extract containing the fusion protein. Nanoparticle synthesis was also done using desalted samples (removal of medium components) as well as enriched fractions from ion exchange chromatography purification. In all cases, palladium, gold and palladium-gold nanoparticles were successfully synthesized with good particle size for catalysis applications, control of diameter, and lack of other metal precipitants, respectively.

This work illustrates that metallic nanoparticles can be synthesized using the soluble cell extract containing the fusion protein without extensive purification or cleavage steps.

## **Acknowledgements**

First of all, I would like to thank my mom, Gioconda and my sisters, Sara and Carolina. Without your never-ending love throughout my whole life, I would not be where I am today. I know it has not been easy being away for almost 6 years, and I am incredibly grateful for the support you have given me in every step of the way.

To the love of my life, Rudra, thank you for always encouraging me to be a better version of myself and for your love and support (in and out of the lab) for the last 3 years. Thank you to Dr. Beitle, the best advisor ever, for being so patient, optimistic and teaching me so much.

I would also like to thank Dr. Nicholas Bedford, for all the help provided with the nanoparticles, and Dr. Lauren Greenlee and Dr. Roger Koeppel for being part of my committee. Thank you to Dr. McKinzie Fruchtl for your help with the fed-batch fermentation.

## Table of Contents

### 1. Introduction

1.1. Peptides.....	1
1.2. Metal binding peptide.....	1
1.3. Nanoparticles.....	2
1.4. Reduction methods for nanoparticle synthesis.....	2
1.5. Recombinant nanoparticles.....	2
1.6. <i>Escherichia Coli</i> and Green Fluorescent Protein (GFP <sub>UV</sub> ) .....	3
1.7. Polymerase Chain Reaction (PCR) .....	4

### 2. Materials and Methods

2.1. Design of primers for SOE PCR.....	6
2.2. Recombinant expression vector construction of MBP-GFP.....	7
2.3. Fed-batch fermentation.....	9
2.4. Desalting and purification.....	10
2.5. Other methods.....	10
2.6. Nanoparticles synthesis.....	11
2.7. Determination of size of nanoparticles.....	12

### 3. Results and discussion

3.1. Recombinant expression vector construction of MBP-GFP.....	13
3.2. Fed-batch fermentation.....	13
3.3. Ion-exchange chromatography and fluorescence analysis.....	15
3.4. Nanoparticle characterization.....	17
3.4.1. Synthesis with crude clarified lysate.....	17
3.4.2. Synthesis with desalted clarified lysate.....	19
3.4.3. Synthesis with desalted and purified fractions.....	22

### 4. Conclusions.....

### 5. References.....

### 6. Appendix.....

## List of Tables and Figures

<b>Figure 1.</b> General structure of an amino acid.....	1
<b>Table 1.</b> List of primers.....	6
<b>Figure 2.</b> Illustration of the cloning by splicing by overlap extension PCR strategy.....	7
<b>Figure 3.</b> Temperature gradient for SOE PCR.....	8
<b>Figure 4.</b> Schematic illustration of the plasmid construction.....	9
<b>Figure 5.</b> 1.2% agarose gel of the PCR product MBP-GFP <sub>UV</sub> .....	13
<b>Figure 6.</b> Growth profile of E. coli containing the MBP-GFP <sub>UV</sub> during fed-batch fermentation.....	14
<b>Figure 7.</b> SDS-PAGE gel.....	15
<b>Figure 8.</b> SDS-PAGE gel.....	16
<b>Figure 9.</b> Ion-exchange chromatography of MBP-GFP <sub>UV</sub> .....	16
<b>Figure 10.</b> a) TEM image of Pd <sup>0</sup> nanoparticles prepared with crude extract, b) size distribution histogram.....	17
<b>Figure 11.</b> Elemental analysis of the synthesis sample.....	18
<b>Figure 12.</b> a) TEM image of the Pd nanoparticles with desalted sample, b) size distribution histogram.....	19
<b>Figure 13.</b> a) HAADF image of the Pd nanoparticles with desalted sample, b) size distribution histogram.....	20
<b>Figure 14.</b> TEM analysis of Au nanoparticles with desalted sample, b) size distribution histogram.....	20
<b>Figure 15.</b> a) TEM analysis of PdAu nanoparticles with desalted sample, b) size distribution histogram.....	21

**Figure 16.** HAADF image of PdAu nanoparticles with desalted sample.....21

**Figure 17.** a) TEM image of the Pd nanoparticles with purified sample, b) size distribution histogram.....22

**Figure 18.** a) HAADF image of PdAu nanoparticles with purified sample, b) size distribution histogram.....23

## 1. Introduction

### 1.1. Peptides

A peptide is a small protein with a specific sequence of amino acid residues. There is a total pool of 20 different natural amino acids that proteins or peptides are built from. All the common amino acids (except for proline) have the same general structure, where there is a central carbon atom ( $C_{\alpha}$ ) that is covalently bonded to an amino group ( $NH_2$ ), a carboxyl group ( $COOH$ ), a hydrogen atom and a side group ( $R$ )<sup>1</sup>.

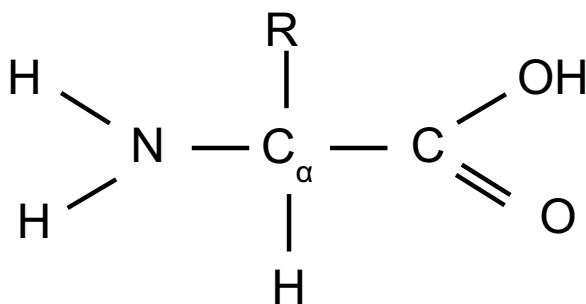


**Figure 1.** General structure of an amino acid <sup>1</sup>

### 1.2. Metal binding peptide

The sequence used for this work is

TSNAVHPTLRHLGGGGTSNAVHPTLRHLGGGGTSNAVHPTLRHLM. It contains the TSNAVHPTLRHL domain, which is a known palladium binding sequence ( $Pd4$ )<sup>2</sup>. Also, four glycine spacers are used to link the  $Pd4$  domains, a common practice when concatenating amino acid sequences<sup>3</sup>. This peptide can be used to synthesize palladium and gold nanoparticles for a variety of catalysis applications<sup>4</sup>. The  $Pd4$  peptide has histidine ( $H$ ) residues at the six and eleven positions, which are expected to help anchor the peptide to metallic surfaces<sup>5</sup>.

### **1.3.Nanoparticles**

By definition, nanotechnology is the science that deals with matter at the scale of 1 billionth of a meter ( $10^{-9}$  m), as well as the study of the modification of matter at the atomic and molecular scale<sup>6</sup>. Nanoparticles are “the most fundamental components in the fabrication of a nanostructure, and are far smaller than the world of everyday objects, but bigger than an atom or a simple molecule that are governed by quantum mechanics”<sup>6</sup>. Most nanoparticles are between the sizes of 1 and 100 nm<sup>7</sup>. Metallic nanoparticles are widely utilized in biomedical sciences and engineering<sup>7</sup>. The properties of metallic nanoparticles can have significant advantages over bulk metals, such as lower melting points and higher specific surface areas<sup>6</sup>.

### **1.4.Reduction methods for nanoparticle synthesis**

Among the liquid phase synthetic methods for nanoparticles there are liquid/liquid and sedimentation methods<sup>6</sup>. Chemical reduction method is considered one of the liquid/liquid methods and includes polyol, organic acids, sodium borohydride and sugar as materials involved in synthesis<sup>6</sup>. This chemical reduction method has many advantages that include the use of simple equipment and it has a high yield of nanoparticles with a low cost and little time<sup>6</sup>. The basic principle of this method relies on the reduction of the metal ions to their 0 oxidation states, in the case of palladium,  $\text{Pd}^{2+} \rightarrow \text{Pd}^0$ .

### **1.5. Recombinant nanoparticles**

Nanoparticles synthesized from recombinantly produced proteins show excellent potential for a wide variety of nanotechnology applications<sup>8</sup>. Bio inspired inorganic nanomaterials have the potential to create novel therapeutics, drug delivery systems and catalysts<sup>2</sup>. Nanoparticles made by peptide-directed synthesis are an example of novel bio inspired materials since nanoparticle

morphology is dictated by a biological component. Examples of present recombinant nanoparticles include PLGA nanoparticles to induce the killing of *Leishmania*<sup>9</sup> and high-density lipoprotein Nanoparticles<sup>10</sup>.

Traditional methods used for synthesis of nanoparticles involve very energy consumptive conditions, so the use of peptides for this purpose is considered a sustainable alternative<sup>11</sup>.

Despite the potential of recombinant nanoparticle platforms, the number of identified recombinant proteins suitable for nanoparticle synthesis applications is very small. Most of the literature describes the use of peptides that are synthesized via solid phase chemistry. Indeed, to date less than 20 references on peptides derived from recombinant sources have been used to direct nanoparticle synthesis. Also, to our knowledge no reference describes the use of a peptide fused to either the N- or C- terminus of a reporter protein to direct nanoparticle synthesis.

There are many proposed advantages to the use of a recombinant platform for nanoparticle synthesis when compared to the use of peptides chemically synthesized. These include cost effectiveness, homogeneity and easy modification<sup>8</sup>. Other features may be incorporated in the construction which allows for the quantification of the product, since traditional techniques like SDS PAGE and mass spectroscopy require additional effort to track the metal binding peptide through the bioprocess.

### **1.6. *Escherichia Coli* and Green Fluorescent Protein (GFP<sub>UV</sub>)**

*Escherichia coli* is widely used for protein expression for a variety of reasons. *E. coli* is inexpensive, it is relatively simple to grow and it has well-known genetics<sup>12</sup>. The media can be

made with easily accessible and cheap components<sup>13</sup>. Also, the transformation protocol with external DNA is very simple and straightforward. Other characteristic that makes *E.coli* very favorable to use is that fermentation processes at large scales exist and high cell densities are achieved in industry<sup>14</sup>. The main disadvantage of using *E.coli* is its inability to perform post translational modifications, and potential issues of product isolation<sup>15</sup>.

The reporter protein GFP<sub>UV</sub> has plenty of useful applications. The most noticeable property is its fluorescence, which can be used to monitor upstream and downstream processing<sup>16</sup>. In addition, GFP<sub>UV</sub> has a stability that is considered an important advantage when used as a fusion partner<sup>16</sup>. It is also easily purified via Immobilized Metal Affinity Chromatography and Aqueous Two Phase Extraction<sup>17</sup>.

### **1.7. Polymerase Chain Reaction (PCR)**

The polymerase chain reaction (PCR) is a molecular biology technique to amplify a piece of DNA, generating thousands to millions of copies of the DNA sequence<sup>18</sup>. There are a few components that are indispensable for PCR<sup>18</sup>:

- Polymerases, which are enzymes that able to put together DNA building blocks.
- Nucleotides consisting of the four bases adenine, thymine, cytosine and guanine, which are referred to as DNA building blocks.
- Primers or small fragments of DNA, to initiate the PCR reaction.
- Original fragment of DNA, that serves as the template.

There are three basic steps for PCR: denaturation, annealing and extension. In denaturation, the two-stranded template DNA is heated at a high temperature (~90-98°C) to separate it into single

strands<sup>18</sup>. In annealing, the primers attach to the DNA template strands at a lower temperature (~72°C). In extension, a new complimentary copy strand of DNA is made using the polymerase enzyme by adding nucleotides to the end of the annealed primers<sup>18</sup>. These three steps are repeated between 20-40 cycles. Splicing by overlap extension PCR (SOE PCR) is a method in which PCR products that are made to share a common sequence at one end are recombined or spliced together without additional nucleotides typical of restriction cloning<sup>19</sup>.

## 2. Materials and Methods

### 2.1. Design of primers for SOE PCR

The sequence of the desired metal binding peptide (MBP) is TSNAVHPTLRHLGGGGTSNAVHPTLRHLGGGGTSNAVHPTLRHLM. A methionine residue was added in the C-terminus of the peptide in order to allow, if desired, cyanogen bromide cleavage of the peptide once it is expressed.

A DNA fragment encoding the MBP was designed according to the codon preference of *E. coli* and was purchased from Integrated DNA Technologies (Coralville, IA). Using a three step PCR scheme, as shown in Figure 2, an MBP-GFP<sub>UV</sub> synthetic gene was created. In the first step, an *NcoI* restriction site is introduced in the 5' end of the MBP with primer Forward 1 along with GFP<sub>uv</sub> in the 3' end with the primer Reverse 1. In step 2, the MBP overlap region is introduced in the 5' end of GFP<sub>uv</sub> using the primer Forward 2 and Histidine 6 tag with an *EcoRI* restriction site in the 3' end using the primer Reverse 2. The two PCR products were spliced together in a third PCR using the Forward 1 and Reverse 2 primers. The primers used in the PCRs are listed in Table 1.

**Table 1.** List of primers

Forward 1	5'-GACGGTAGAACCATGGGTACTTCCAATGCCGTCCA-3'
Reverse 1	5'-GTGAAAAGTTCTTCTCCTTTACTCATTAAAGTGACGCAAGGTCGG-3'
Forward 2	5'-CCGACCTTGCGTCACTTAATGAGTAAAGGAGAAGAAGCTTTTCAC-3'
Reverse 2	5'-TGCGAATTCTTAATGGTGATGGTGATGGTGTGGTTGTAGAGCTCATC-3'

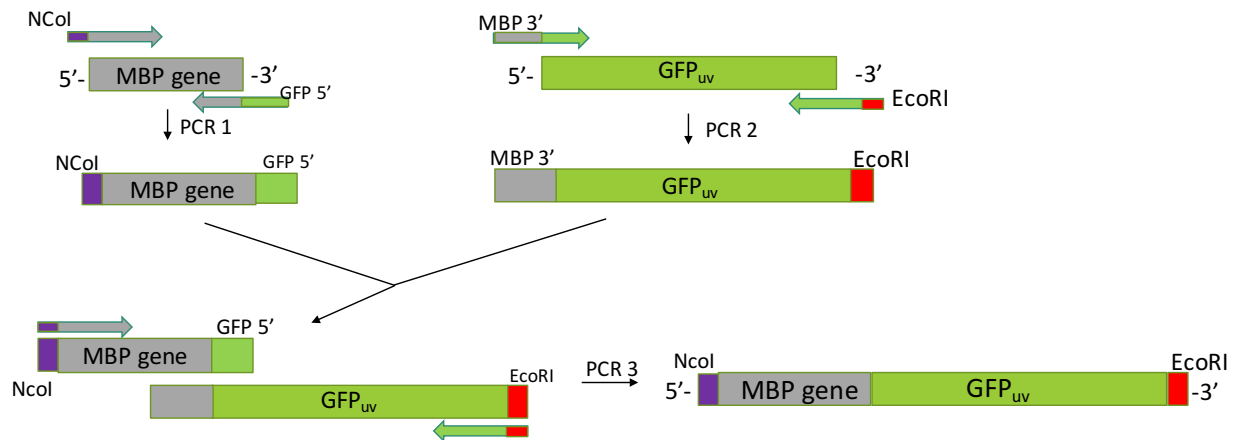


**Figure 2.** Illustration of the cloning by splicing by overlap extension PCR strategy

## 2.2.Recombinant expression vector construction of MBP-GFP<sub>uv</sub>

Splicing by overlap extension polymerase chain reaction (SOE PCR) was performed using the Q5® High-Fidelity 2X Master Mix 25 µL reaction protocol from New England Biolabs (Ipswich, MA). The components that were mixed for the PCR reaction were: 12.5 µL of the Q5® Master Mix, 1.25 µL forward primer, 1.25 µL reverse primer, 5 µL of the template DNA and 5 µL of nuclease-free water. The final PCR product contains the MBP fused to GFP<sub>UV</sub> from Clontech (Mountain View, CA).

The PCR product and pBAD plasmid were double digested using *EcoRI*-HF® and *NcoI*-HF® restriction enzymes from New England Biolabs. Both products were recovered using a two-tier 1.2% agarose FlashGel cassette and Recovery buffer from Lonza (Rockland, ME).

Finally, ligation of the digested PCR product and the digested pBAD occurred overnight using T4 DNA Ligase enzyme and T4 DNA Ligase Reaction buffer (New England Biolabs) at 14°C. The recombinant plasmid construction is illustrated in Figure 4.

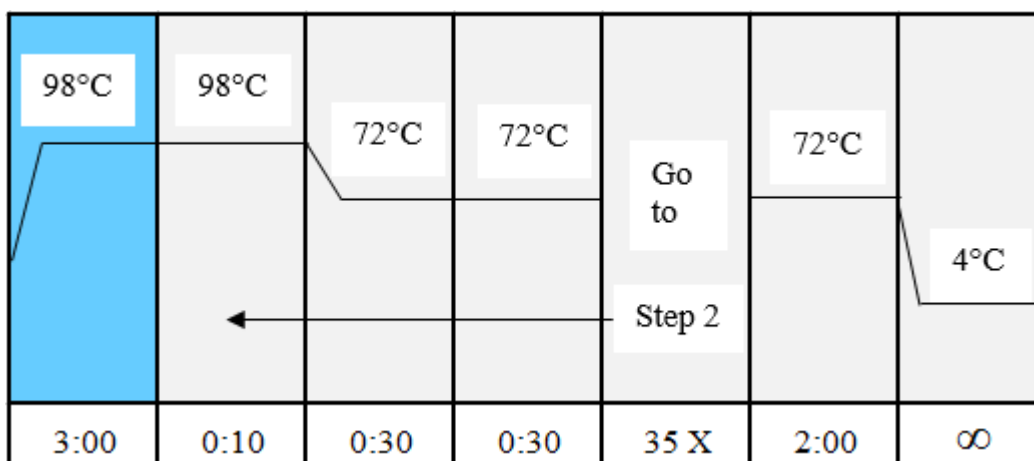


**Figure 3.** Temperature gradient for SOE PCR

The ligation product was transformed using the heat shock method. Using 50  $\mu\text{L}$  of 10-Beta *E. coli* competent cells from New England Biolabs, 5  $\mu\text{L}$  of the ligation product was added and the mixture was placed in ice for 30 minutes. The cells were heat shocked at 42°C for 30 seconds, then placed on ice for 5 minutes. 950  $\mu\text{L}$  of SOC Outgrowth medium was added to the cells and then incubated in a shaker for 60 minutes at 37°C. The cells were plated on LB agar media containing 50  $\mu\text{g}/\text{mL}$  ampicillin and 2  $\text{mg}/\text{mL}$  arabinose. The plates were incubated overnight at 37°C and the product was checked for green fluorescence using UV light.

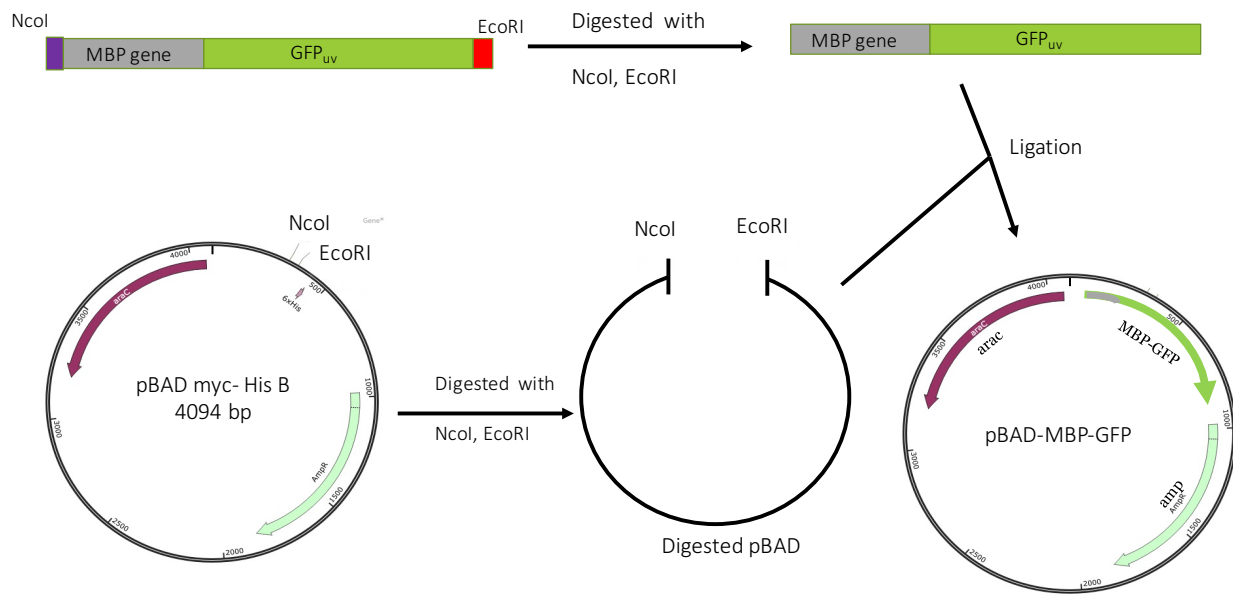


**Figure 4.** Schematic illustration of the plasmid construction

### 2.3. Fed-batch fermentation

A single colony of the transformed cells was inoculated into 5 mL of Lysogeny Broth (LB) media and 50 µg/mL ampicillin and incubated overnight in a shaker at 37°C. Then, 1 mL of this culture was inoculated in a shake flask containing 100 mL of LB media and 50 µg/mL ampicillin and incubated overnight. Once the inoculum for the fed batch fermentation was prepared in the shake flask, 50 mL of the overnight culture was added to 1.5 L of LB media in a 3 L Applikon bioreactor with BioXpert Advanced software. The bioreactor was fed with 500 g/L sterilized glucose solution. The temperature in the reactor was maintained at 37°C using a heating jacket and cooling loop. The pH was maintained at 6.8 using 7 M of NH<sub>4</sub>OH. Bugeye optical density sensor (BugLab, Foster City, CA) was used for measuring the optical density. After 16 hours of fermentation, the culture was induced with 10 mM arabinose. Four hours after induction, the fermentation was stopped and the cells were harvested by centrifugation at 5000 x g and 3 °C and were stored at -80°C.

## **2.4.Desalting and purification**

For some samples, excess salts in the clarified lysate were removed using a 3.5 kDa MWCO dialysis membranes from Spectrum Laboratories (Rancho Dominguez, CA). The clarified lysate was processed using an ÄKTA FPLC System from Amersham Biosciences. A HiTrap DEAE FF column from GE Healthcare was equilibrated with IEX DEAE Buffer A (25 mM Tris-HCl, pH=8). The clarified lysate (20 mL) was loaded at a flow rate of 0.5 mL/min. The column was washed with 20 column volumes (CV) at a flow rate of 1 mL/min with the Buffer A previously mentioned. After the column was washed and lysate loaded, enrichment proceeded via a stepwise elution with IEX DEAE Buffer B (25 mM Tris-HCl, 1 M NaCl, pH=8). Fractions of 3 mL were collected, and the ones that fluoresced green under UV light were analyzed using SDS-PAGE gel and a fluorimeter.

## **2.5. Other Methods**

After the cells were harvested, 7 grams of pellet were resuspended in 40 mL of deionized water and then lysed on ice using Q125 Sonicator at 40% amplitude with 10 seconds pulse and 15 seconds rest period for a total of 20 minutes.

The total concentration of protein in the clarified lysate was determined using the DC<sup>TM</sup> Protein Assay from Bio-Rad (Hercules, CA) following the instructions from the manufacturer. The standard curve that was used, which was made using bovine serum albumin, can be found in the Appendix.

Densitometric analysis was performed using ImageJ software with an 12.5% sodium dodecyl polyacrylamide gel electrophoresis (SDS-PAGE) band corresponding to the molecular weight of the MBP-GFP<sub>UV</sub>.

The fractions collected from IEX chromatography were used for fluorometric measurements using a RF-Mini 150 Recording Fluorometer from Shimadzu (Kyoto, Japan) with excitation and emission filters of 395 nm and 510 nm, respectively. The instrument was zeroed with deionized water and a maximum value of 1000 RFU (relative fluorescence units) with a reference sample of highly concentrated GFP<sub>UV</sub>.

## **2.6. Nanoparticle synthesis and characterization**

The protocol used for synthesis of nanoparticles was adapted from previous work. Palladium nanoparticles were synthesized by first mixing for 30 minutes at room temperature: 750  $\mu\text{L}$  of double distilled water, 230  $\mu\text{L}$  of the clarified lysate and 5  $\mu\text{L}$  of 0.1 M potassium tetrachloropalladate ( $\text{K}_2\text{PdCl}_4$ ). After Pd complexation, 40  $\mu\text{L}$  of 1.0 M sodium borohydride ( $\text{NaBH}_4$ ) was added to reduce the  $\text{Pd}^{2+}$  to  $\text{Pd}^0$  nanoparticle. The particles were then left undisturbed for 1 hour prior to testing and characterization.

The palladium-gold (PdAu) nanoparticles were synthesized by adding gold at a 1:1 ratio with palladium. In this case, 750  $\mu\text{L}$  of double distilled water, 230  $\mu\text{L}$  of the clarified lysate, 2.5  $\mu\text{L}$  of 0.1 M potassium tetrachloropalladate ( $\text{K}_2\text{PdCl}_4$ ) and 2.5  $\mu\text{L}$  of 0.1 M hydrogen tetrachloroaurate ( $\text{HAuCl}_4$ ). This mix was left undisturbed for 30 minutes at room temperature, before adding 40  $\mu\text{L}$  of 1.0 M sodium borohydride. The particles were tested and characterized 1 hour later.

TEM samples were prepped by placing droplet of as synthesized material on Cu TEM grids coated with a thin layer of C (Ted Pella, Inc.). After one minute, the droplet was wicked away with a Kimwipe, leaving a non-aggregated layer of physisorbed nanoparticles. Images and electron dispersive spectroscopy were performed in scanning transmission mode operating at 300 kV.

### **2.7.Determination of size of nanoparticles**

The analysis of the TEM images obtained of the nanoparticles was done using ImageJ software. Using the area of the particles measured from ImageJ, the diameter of each one was calculated with the formula  $A=\pi r^2$ , where  $d=2r$ .

### 3. Results and discussion

#### 3.1.Recombinant expression vector construction of MBP-GFP<sub>uv</sub>

The PCR product of MBP-GFP<sub>uv</sub> has a size of 936 bp. A DNA fragment between 800 and 1200 bp was obtained using a single-tier 1.2% agarose Lonza's FlashGel™ Cassette as shown in Figure 5.

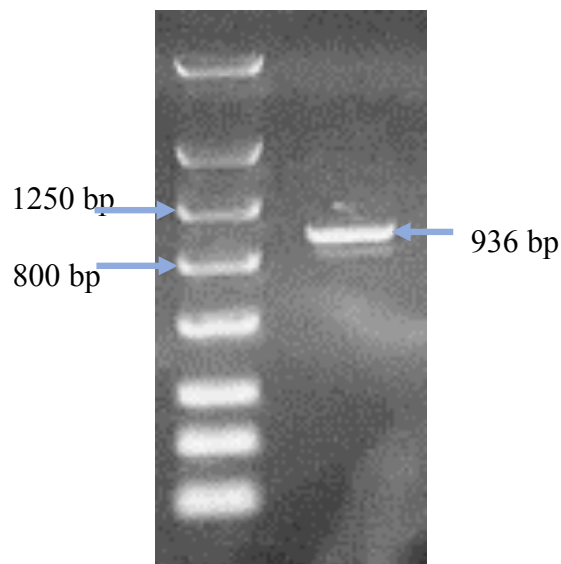


**Figure 5.** 1.2% agarose gel of the PCR product MBP-GFP<sub>UV</sub>

The recombinant plasmid was transformed into 10-beta *E. coli* cells. Plated cells were visibly green under UV light after overnight growth on an LB agar plate containing 50 µg/mL ampicillin and 2 mg/mL arabinose (data not shown).

#### 3.2.Fed-batch fermentation

Fed-batch fermentation was performed in order to reach high cell density. Figure 6 shows the plot of OD<sub>600</sub> as a function of time in hours. A terminal OD<sub>600</sub> of 22.1 was reached during the fed-batch fermentation run which yielded a total of 75 g cell pellet.

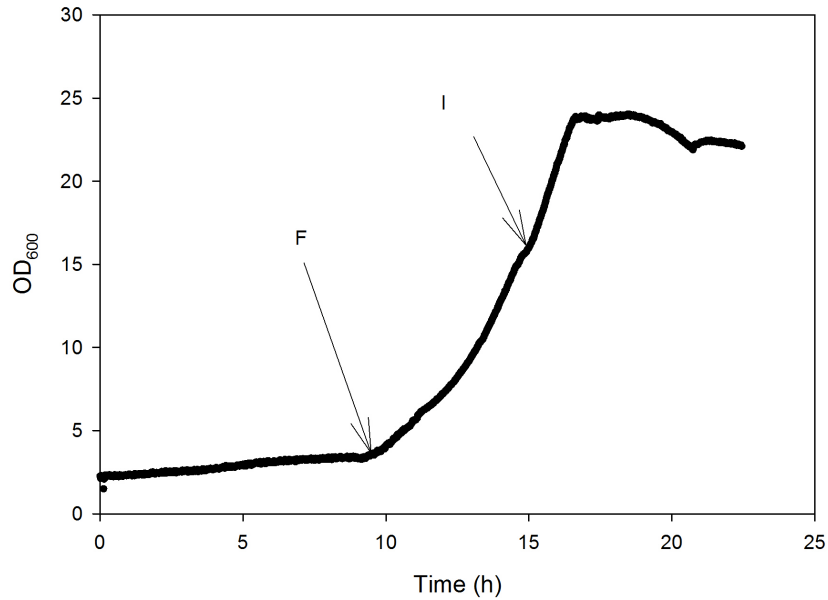


**Figure 6.** Growth profile of *E. coli* containing the MBP-GFP<sub>UV</sub> during fed-batch fermentation. “F” indicates the start of the feed into the bioreactor and “I” indicates the time of the induction.

Figure 7 is an SDS-PAGE gel of the clarified lysate obtained from fed-batch fermentation. Using total protein assay, the protein concentration was estimated to be 7.4 mg/mL. It was determined using densitometry that the fusion protein content was approximately 11%.

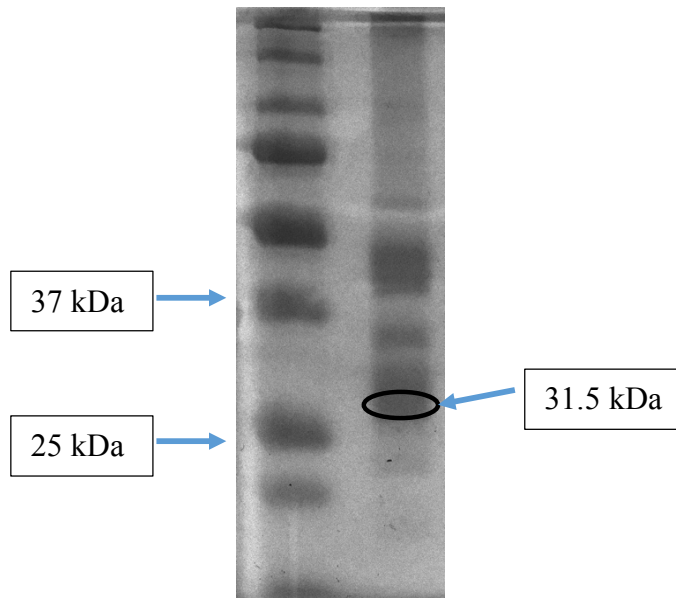


**Figure 7.** SDS-PAGE gel. Lane 1, molecular weight marker. Lane 2, clarified lysate of crude extract, the circle marking the band corresponding to MBP-GFP<sub>UV</sub>

### 3.3. Ion-exchange chromatography and fluorescence analysis

Since the SDS-PAGE gel seen on Figure 8 was somewhat qualitative because the band presumed to be MBP-GFP may be several proteins of similar molecular weight, a fluorescence analysis was done on the IEX fractions corresponding to peaks “A”, “B” and “C” seen on Figure 8. The fraction corresponding to peak B was expected to have the highest fluorescence based on visualization under UV light, and it was confirmed by the fluorometer measurements specified on Figure 9. The fraction with 525 RFUs was used in later experiments to synthesize nanoparticles.

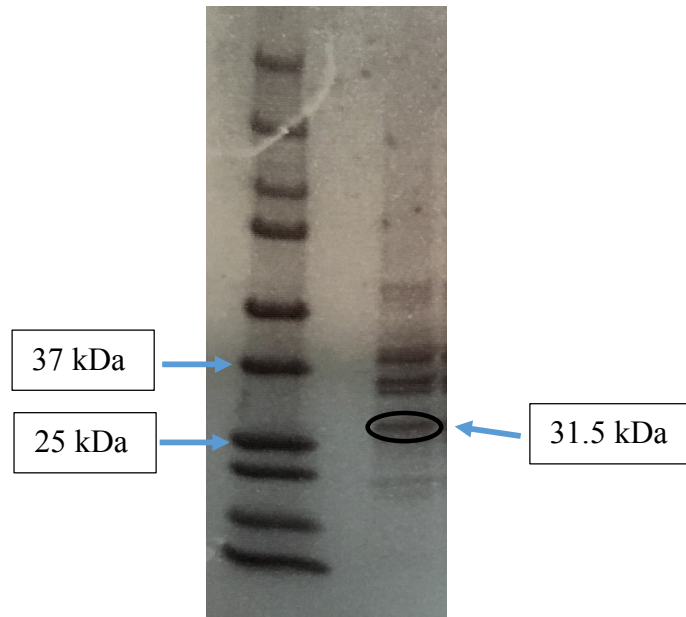


**Figure 8.** SDS-PAGE gel. Lane 1, molecular weight marker. Lane 2, IEX product fraction corresponding to peak “B”, the circle marking the band corresponding to MBP-GFP<sub>UV</sub>

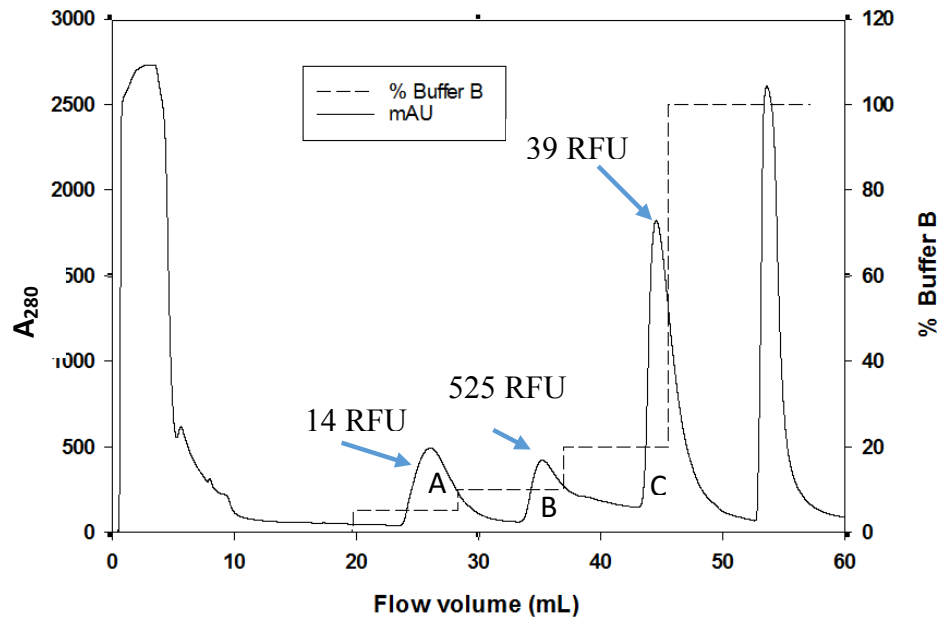


**Figure 9.** Ion-exchange chromatography of MBP-GFP<sub>UV</sub>

### 3.4. Nanoparticle synthesis and characterization

#### 3.4.1. Synthesis with crude clarified lysate

The synthesis of nanoparticles was attempted with the crude clarified lysate obtained after fed batch fermentation. The synthesis was successful in the fact that small spherical Pd nanoparticles with an average size of  $1.18 \text{ nm} \pm 0.21 \text{ nm}$  were obtained, as seen in the size distribution histogram in Figure 10b. However, there were a lot of extra particulate matter in the sample. In Figure 11, it can be seen that there are larger particles in the sample that appear to be magnesium oxide (MgO), which led to believe that the magnesium from the medium was reduced with the Pd, but then oxidizes since the synthesis is done in aqueous solution.

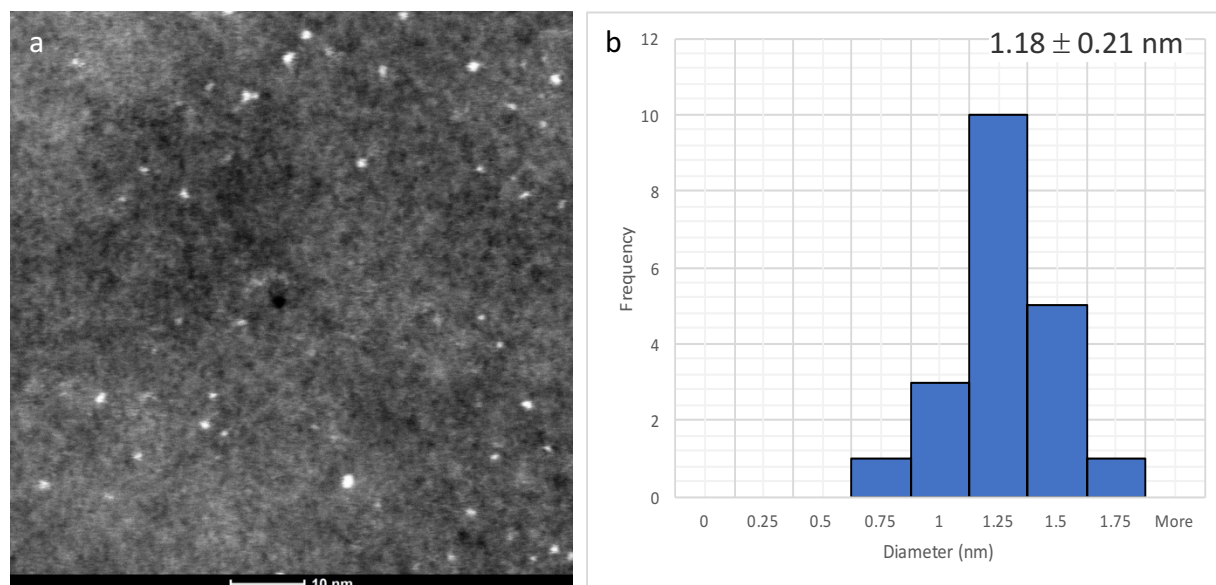


**Figure 10.** a) TEM image of the Pd nanoparticles with the crude cell lysate, b) size distribution histogram

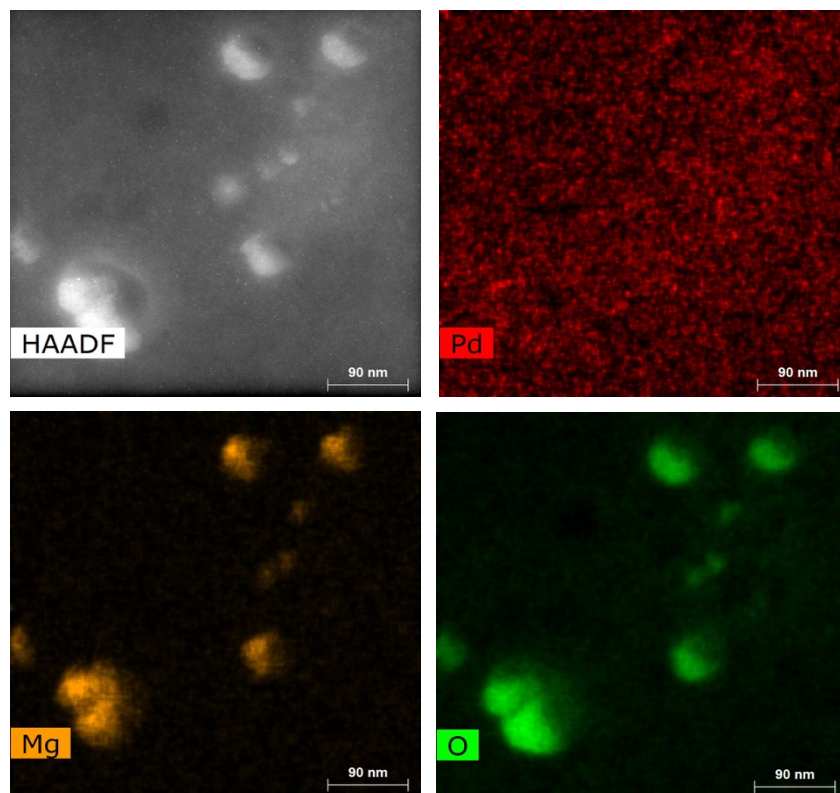


**Figure 11.** Elemental analysis of the sample

### 3.4.2. Synthesis with desalted clarified lysate

After seeing the results from the first synthesis attempt, it was concluded that a possible solution would be to desalt the sample to remove the extra components from the medium. The palladium particles obtained with the desalted sample had a bigger average diameter than the previously synthesized particles with the crude extract. Also, MBP-GFP<sub>UV</sub> was used successfully to synthesize gold and bimetallic palladium-gold nanoparticles. The Pd and Au nanoparticles are consistent with the previously made materials using peptides made by solid phase synthesis.

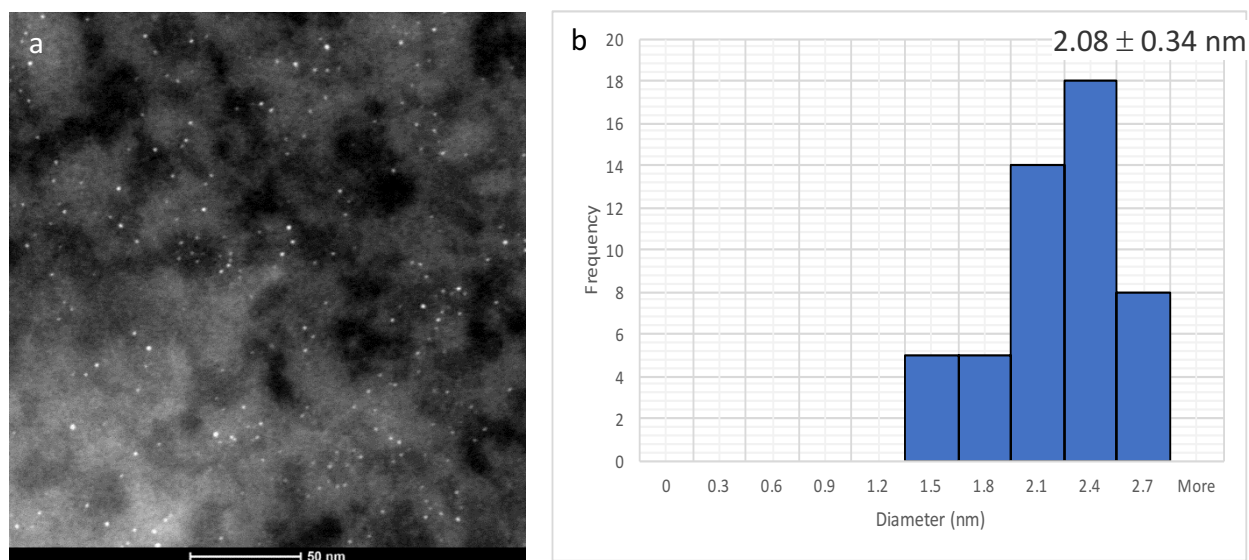


**Figure 12.** a) TEM image of the Pd nanoparticles with desalted sample, b) size distribution histogram

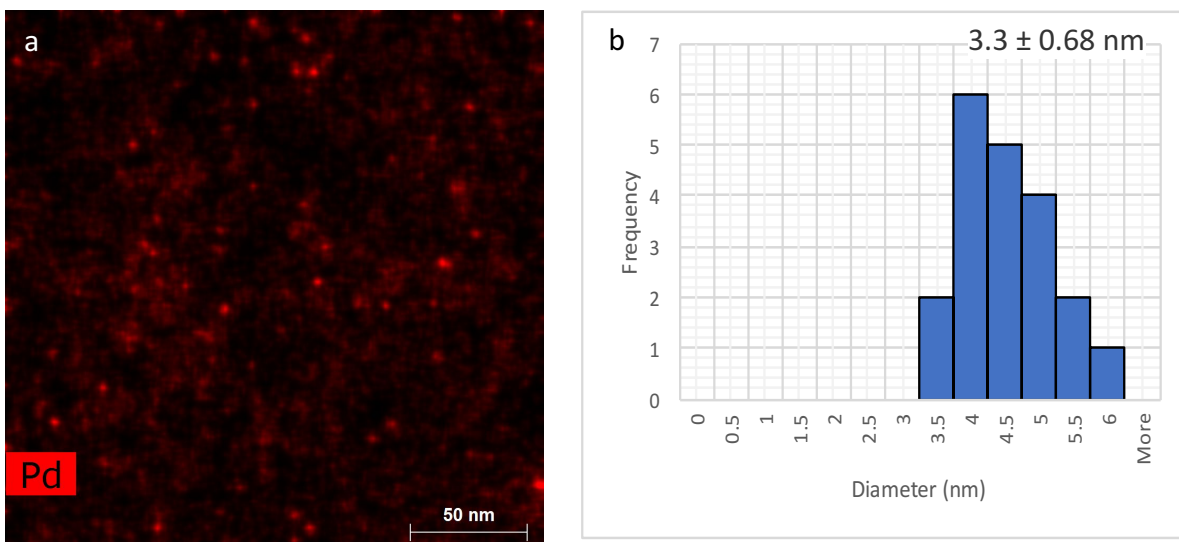


**Figure 13.** a) HAADF image of the Pd nanoparticles with desalted sample, b) size distribution histogram

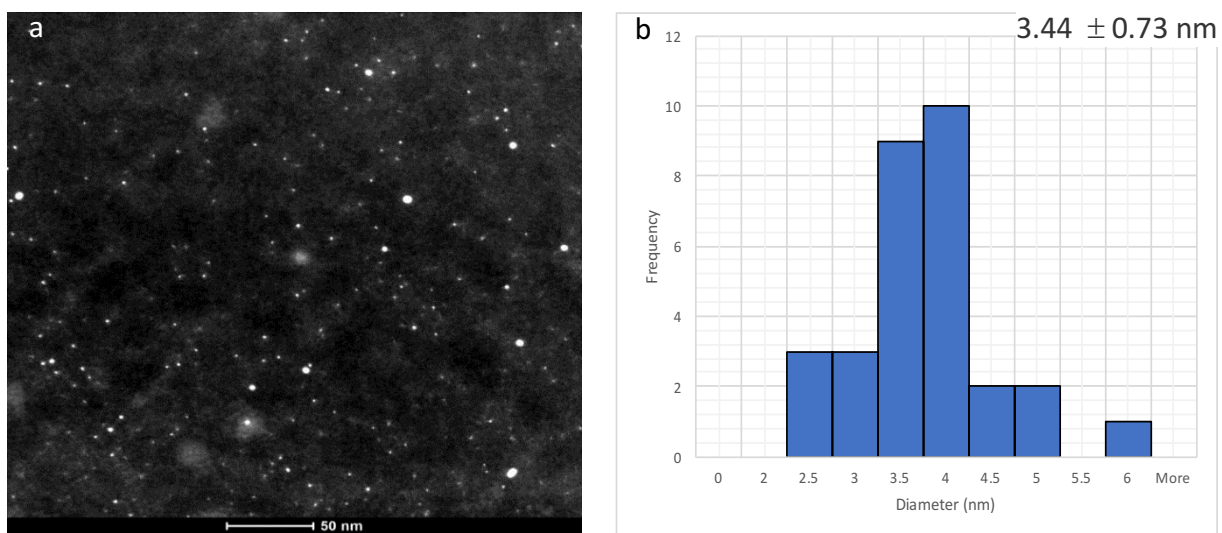


**Figure 14.** a) TEM image of the Au nanoparticles with desalted sample, b) size distribution histogram

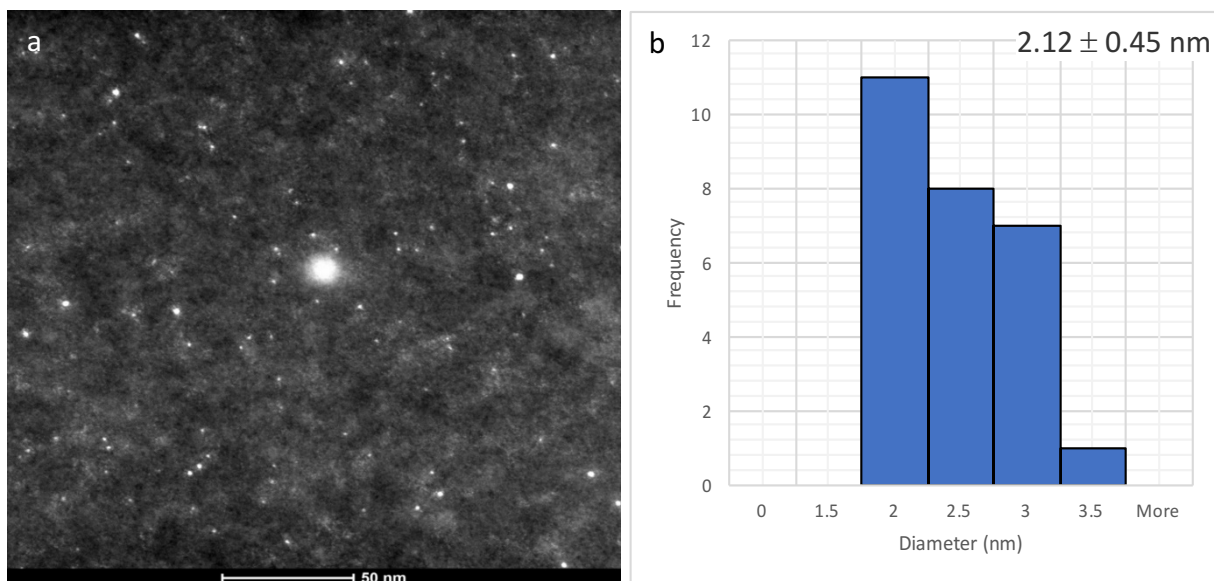


**Figure 15.** TEM analysis of PdAu nanoparticles with desalted sample, b) size distribution histogram

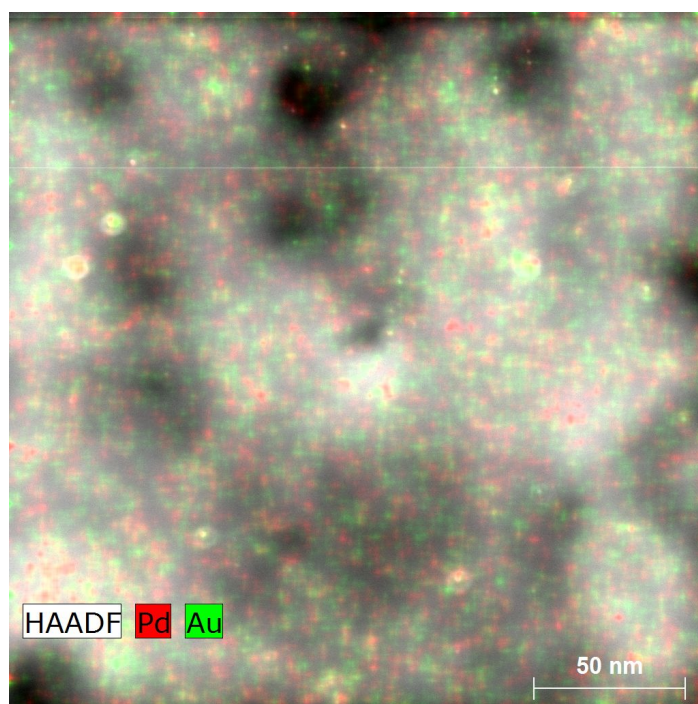


**Figure 16.** HAADF image of PdAu nanoparticles with desalted sample

### 3.4.3. Synthesis with desalted and purified fractions

The nanoparticle synthesis was done using enriched samples from IEX chromatography.

Palladium nanoparticles with an average diameter of  $2.6 \pm 0.7$  nm were synthesized. In addition,

PdAu nanoparticles with an average diameter of  $2.1 \pm 0.7$  nm were obtained.

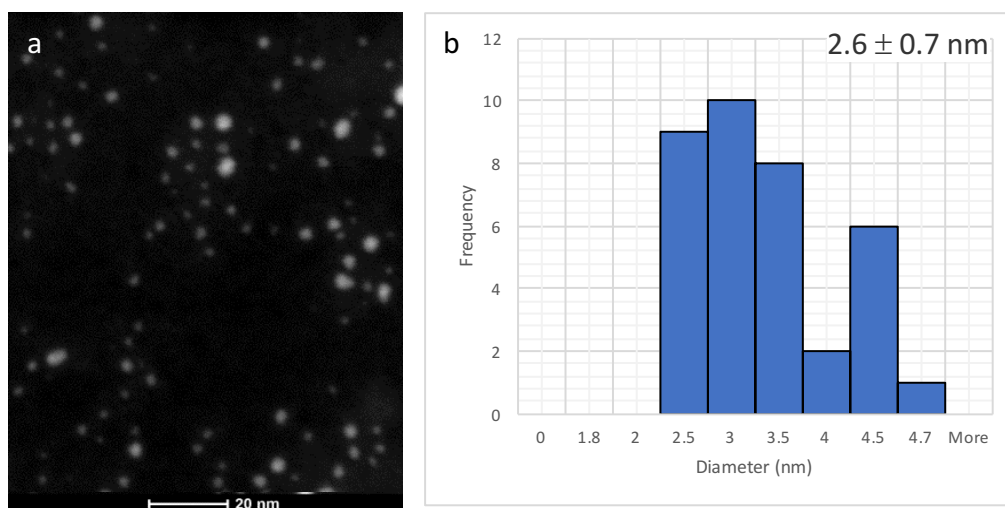


**Figure 17.** a) TEM image of the Pd nanoparticles with purified sample, b) size distribution histogram

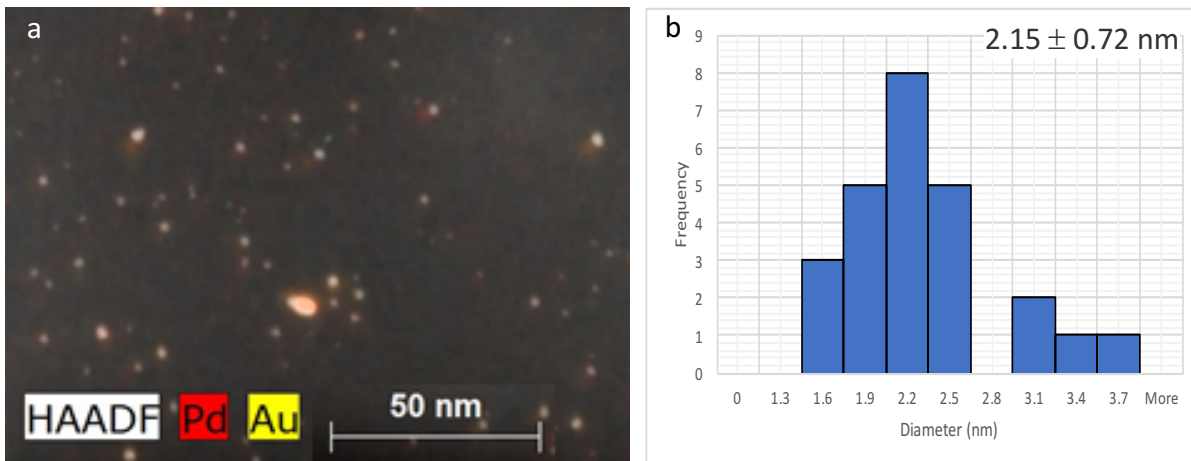


**Figure 18.** a) HAADF image of PdAu nanoparticles with purified sample, b) size distribution histogram

#### **4. Conclusions**

Nanoparticles synthesized using peptides that are produced recombinantly show potential for catalytic applications, but require some means of cost effective synthesis. The use of recombinantly produced peptides for nanoparticle synthesis represents a more sustainable method for large-scale production of these nanoparticles. This work has shown that nanoparticles of gold, palladium, and gold-palladium can be synthesized with three copies of Pd4 fused to GFP<sub>UV</sub>. It motivates a comprehensive examination of the purity requirements of the peptide to effectively direct nanoparticle synthesis, because the degree of purity and properties of the nanoparticles has not been thoroughly correlated. This work demonstrated that nanoparticles can be synthesized with soluble cell extract, desalted samples, and partially enriched samples. Determining the tolerance of byproducts with regard to catalytic efficiency would complete the investigation, accompanied by an economic analysis that would encompass MBP synthesis, nanoparticle synthesis, and quality of catalytic activity.

## 5. References

1. Pandey, R. B. *et al.* Adsorption of peptides (A3, Flg, Pd2, Pd4) on gold and palladium surfaces by a coarse-grained Monte Carlo simulation. *Phys. Chem. Chem. Phys.* **11**, 1869 (2009).
2. Bedford, N. M. *et al.* Elucidation of Peptide-Directed Palladium Surface Structure for Biologically Tunable Nanocatalysts. 5082–5092 (2015).
3. Dickerson, M. B., Sandhage, K. H. & Naik, R. R. Protein- and peptide-directed syntheses of inorganic materials. *Chem. Rev.* **108**, 4935–4978 (2008).
4. Pacardo, D. B., Sethi, M., Jones, S. E., Naik, R. R. & Knecht, M. R. Biomimetic synthesis of pd nanocatalysts for the stille coupling reaction. *ACS Nano* **3**, 1288–1296 (2009).
5. Nguyen, M. a. *et al.* Direct Synthetic Control over the Size, Composition, and Photocatalytic Activity of Octahedral Copper Oxide Materials: Correlation Between Surface Structure and Catalytic Functionality. *ACS Appl. Mater. Interfaces* 150609095239000 (2015). doi:10.1021/acsami.5b04282
6. Horikoshi, S. & Serpone, N. Introduction to Nanoparticles. 1–24 (2013).
7. Mody, V. V., Siwale, R., Singh, A. & Mody, H. R. Introduction to metallic nanoparticles. 2(4): 282-289
8. Bonde, J. & Bülow, L. Random mutagenesis of amelogenin for engineering protein nanoparticles. *Biotechnol. Bioeng.* **112**, 1319–1326 (2015).
9. Santos, D. M. *et al.* PLGA nanoparticles loaded with KMP-11 stimulate innate immunity and induce the killing of Leishmania. *Nanomedicine Nanotechnology, Biol. Med.* **9**, 985–995 (2013).
10. Rui, M. *et al.* Recombinant high-density lipoprotein nanoparticles containing gadolinium-labeled cholesterol for morphologic and functional magnetic resonance imaging of the liver. *Int. J. Nanomedicine* **7**, 3751–3768 (2012).
11. Briggs, B. D. & Knecht, M. R. Nanotechnology meets biology: Peptide-based methods for the fabrication of functional materials. *J. Phys. Chem. Lett.* **3**, 405–418 (2012).
12. Sørensen, H. P. & Mortensen, K. K. Advanced genetic strategies for recombinant protein expression in Escherichia coli. *J. Biotechnol.* **115**, 113–128 (2005).
13. Rosano, G. L. & Ceccarelli, E. A. Recombinant protein expression in Escherichia coli: Advances and challenges. *Front. Microbiol.* **5**, 1–17 (2014).
14. Wegmuller, S. & Schmid, S. Recombinant Peptide Production in Microbial Cells. *Curr. Org. Chem.* **18**, 1005–1019 (2014).

15. Mukherjee, R. P. Cloning , Fed-Batch Expression And Purification Of A Novel Anti-Candida Peptide And Development Of A Cleavage Resistant Variant Of Green Fluorescence Protein. (2016).
16. Mukherjee, R. P., Beitle, R., Jayanthi, S., Kumar, T. K. S. & McNabb, D. S. Production of an anti-Candida peptide via fed batch and ion exchange chromatography. *Biotechnol. Prog.* **32**, 865–71 (2016).
17. Li, Y. & Beitle, R. R. Protein purification via aqueous two-phase extraction (ATPE) and immobilized metal affinity chromatography. Effectiveness of salt addition to enhance selectivity and yield of GFPuv. *Biotechnol. Prog.* **18**, 1054–1059 (2002).
18. Solanki, G. Polymerase Chain Reaction. *Int. J. Pharmacol. Res.* **2**, 98–102 (2012).
19. Horton, R. M., Cai, Z. L., Ho, S. N. & Pease, L. R. Gene splicing by overlap extension: Tailor-made genes using the polymerase chain reaction. *Biotechniques* **54**, 528–535 (2013).
20. Page, P. M. An introduction to proteins and peptides. 7–16

## 6. APPENDIX

List of 20 amino acids and their notations<sup>20</sup>

Non-polar or hydrophobic R-group	
A	Alanine (Ala)
V	Valine (Val)
L	Leucine (Leu)
I	Isoleucine (Ile)
M	Methionine (Met)
P	Proline (Pro)
F	Phenylalanine (Phe)
W	Tryptophan (Trp)

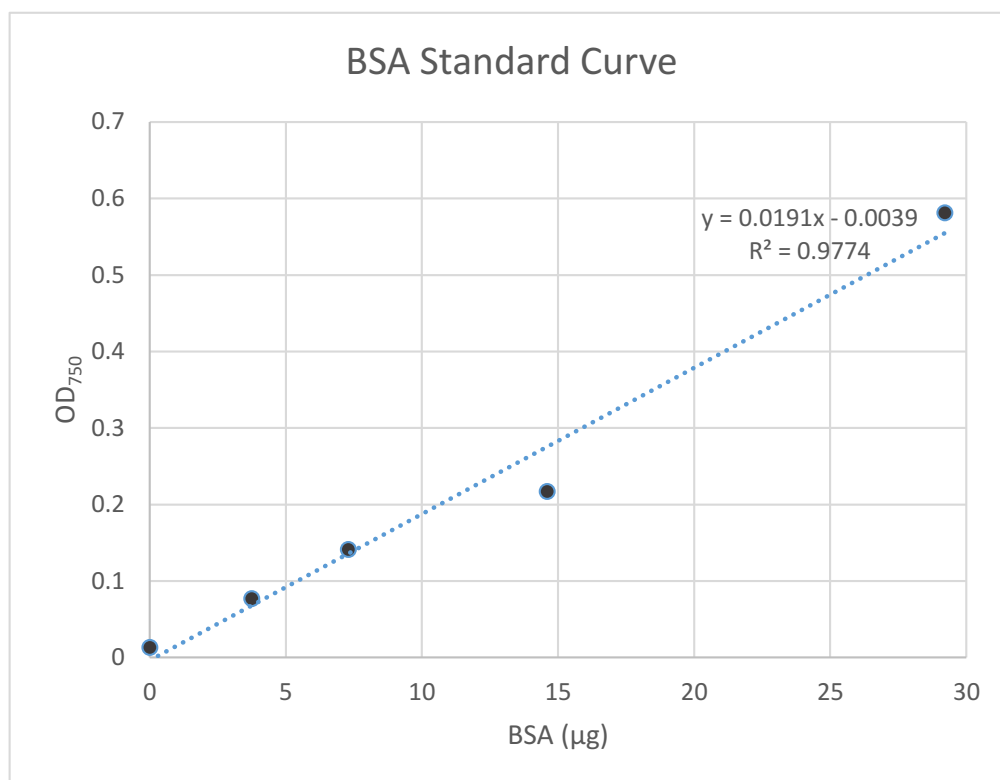
Negatively charged R-groups at pH 6-7	
D	Aspartic Acid (Asp)
E	Glutamic Acid (Glu)

Uncharged or hydrophilic R-groups	
N	Asparagine (Asn)
Q	Glutamine (Gln)
G	Glycine (Gly)
T	Threonine (Thr)
Y	Tyrosine (Tyr)
S	Serine (Ser)
C	Cysteine (Cys)

Positively charged R- groups at pH 6-7	
L	Lysine (Lys)
R	Arginine (Arg)
H	Histidine (His)

BSA Standard curve for DC™ Protein Assay

BSA standard curve					
BSA (uL)	BSA (mL)	BSA (mg/mL)	BSA (mg)	BSA (ug)	OD (750 nm)
0	0	0	0	0	0.013
20	0.02	0.187	0.00374	3.74	0.077
20	0.02	0.365	0.0073	7.3	0.141
20	0.02	0.73	0.0146	14.6	0.217
20	0.02	1.46	0.0292	29.2	0.581



Sample (uL)	OD (750 nm)	Mass (ug)	Concentration (ug/uL)
3.5	0.454	23.973822	6.85
4	0.563	29.6806283	7.42

Determination of the size of Nanoparticles using ImageJ software.

- Palladium nanoparticles (crude extract) (Figure 10)

	Area	Mean	Min	Max		radius (nm)	diameter (nm)
1	2.037	191.336	86	255		0.81	1.61
2	1.443	177.206	98	245		0.68	1.36
3	1.175	199.886	100	255		0.61	1.22
4	1.428	165.375	95	221		0.67	1.35
5	1.041	234.014	185	254		0.58	1.15
6	1.547	201.404	107	254		0.70	1.40
7	0.773	174.423	110	221		0.50	0.99
8	0.55	174.919	137	208		0.42	0.84
9	0.952	196.75	120	245		0.55	1.10
10	1.175	152.443	59	242		0.61	1.22
11	0.416	180	130	206		0.36	0.73
12	1.175	214.937	137	255		0.61	1.22
13	1.71	242.957	190	255		0.74	1.48
14	1.175	160.671	89	220		0.61	1.22
15	1.175	197.848	102	254		0.61	1.22
16	1.041	203.5	151	246		0.58	1.15
17	0.55	193.189	153	220		0.42	0.84
18	0.892	200.283	136	248		0.53	1.07
19	1.175	203.646	124	253		0.61	1.22
20	1.279	220.779	148	254		0.64	1.28

Determination of the size of Nanoparticles using ImageJ software.

- Palladium nanoparticles (desalted) (Figure 12)

	Area	Mean	Min	Max		radius (nm)	diameter (nm)
1	1.765	229.364	138	254		0.75	1.50
2	1.412	105.688	46	166		0.67	1.34
3	3.114	135.206	75	218		1.00	1.99
4	3.807	91.934	37	166		1.10	2.20
5	2.231	119.893	34	222		0.84	1.69
6	2.168	147.465	97	192		0.83	1.66
7	3.807	160.854	66	254		1.10	2.20
8	4.399	181.384	64	254		1.18	2.37
9	3.807	157.606	69	254		1.10	2.20
10	1.349	118.916	71	178		0.66	1.31
11	2.698	114.009	55	187		0.93	1.85
12	5.042	150.805	79	249		1.27	2.53
13	3.227	159.176	70	242		1.01	2.03
14	3.227	127.141	28	240		1.01	2.03
15	2.698	131.556	58	209		0.93	1.85
16	5.635	125.255	57	246		1.34	2.68
17	3.807	110.086	13	220		1.10	2.20
18	3.227	124.457	50	217		1.01	2.03
19	3.807	108.487	35	193		1.10	2.20
20	2.168	92.738	26	168		0.83	1.66
21	1.765	105.414	48	188		0.75	1.50
22	3.807	79.427	17	205		1.10	2.20
23	4.399	167.203	46	254		1.18	2.37
24	2.231	162.802	77	243		0.84	1.69
25	3.58	159.961	75	251		1.07	2.13
26	2.698	188.883	101	254		0.93	1.85
27	5.042	139.938	63	254		1.27	2.53
28	3.227	133	60	218		1.01	2.03
29	5.647	149.114	66	254		1.34	2.68
30	4.286	139.721	45	254		1.17	2.34
31	4.815	139.026	33	254		1.24	2.48
32	1.765	161.021	74	241		0.75	1.50
33	3.58	152.637	82	254		1.07	2.13
34	3.807	190.646	97	254		1.10	2.20
35	3.227	144.086	87	241		1.01	2.03
36	5.647	217.804	141	254		1.34	2.68
37	4.399	219.017	131	254		1.18	2.37
38	3.114	174.138	119	254		1.00	1.99
39	2.698	175.271	100	254		0.93	1.85
40	5.635	196.951	125	254		1.34	2.68
41	4.097	230.375	177	254		1.14	2.28
42	3.227	166.344	100	242		1.01	2.03
43	4.399	150.874	88	232		1.18	2.37
44	3.807	144.884	69	254		1.10	2.20
45	2.168	152.035	88	213		0.83	1.66
46	3.114	113.324	48	184		1.00	1.99
47	3.807	218.291	147	254		1.10	2.20
48	4.815	151.442	65	254		1.24	2.48
49	3.807	93.036	23	170		1.10	2.20
50	2.698	95.472	32	165		0.93	1.85

Determination of the size of Nanoparticles using ImageJ software.

- Palladium nanoparticles image using HAADF (desalted) (Figure 13)

	Area	Mean	Min	Max		radius (nm)	diameter (nm)
1	20.412	31.285	10	57		2.55	5.10
2	7.553	29.689	19	41		1.55	3.10
3	12.043	25.915	11	41		1.96	3.92
4	12.145	30.819	17	47		1.97	3.93
5	11.023	45.662	28	63		1.87	3.75
6	17.81	51.845	25	88		2.38	4.76
7	16.075	38.508	20	62		2.26	4.52
8	14.697	40.58	21	63		2.16	4.33
9	14.493	34.43	15	66		2.15	4.30
10	9.798	37.177	21	59		1.77	3.53
11	11.635	38.303	18	65		1.92	3.85
12	11.431	34.509	16	55		1.91	3.82
13	27.659	50.024	23	87		2.97	5.93
14	22.862	41.449	18	78		2.70	5.40
15	8.981	42.028	23	68		1.69	3.38
16	16.738	28.979	15	50		2.31	4.62
17	15.207	32.383	18	49		2.20	4.40
18	15.411	31.252	16	46		2.21	4.43
19	14.697	40.684	21	69		2.16	4.33
20	16.075	44.514	15	84		2.26	4.52

Determination of the size of Nanoparticles using ImageJ software.

- Gold nanoparticles (desalted) (Figure 14)

	Area	Mean	Min	Max		radius (nm)	diameter (nm)
1	18.992	245.694	110	254		2.46	4.92
2	10.142	244.91	119	254		1.80	3.59
3	12.881	236.215	93	254		2.02	4.05
4	10.142	247.982	126	254		1.80	3.59
5	16.507	213.161	68	254		2.29	4.58
6	12.881	215.931	51	254		2.02	4.05
7	10.142	199.4	59	254		1.80	3.59
8	11.359	253.629	207	254		1.90	3.80
9	7.658	207.377	71	254		1.56	3.12
10	25.863	231.725	72	254		2.87	5.74
11	7.201	167.746	42	254		1.51	3.03
12	7.658	214.646	81	254		1.56	3.12
13	4.361	152.448	42	254		1.18	2.36
14	7.658	134.977	41	254		1.56	3.12
15	6.491	139.09	38	254		1.44	2.87
16	7.658	154.682	52	254		1.56	3.12
17	10.142	174.31	26	254		1.80	3.59
18	7.201	192.447	58	254		1.51	3.03
19	8.621	223.438	114	254		1.66	3.31
20	4.488	157.938	44	254		1.20	2.39
21	9.686	169.683	45	254		1.76	3.51
22	7.201	159.218	39	254		1.51	3.03
23	6.263	157.789	42	254		1.41	2.82
24	7.658	150.868	37	254		1.56	3.12
25	10.142	142.395	40	254		1.80	3.59
26	10.142	144.098	48	254		1.80	3.59
27	10.142	117.28	22	254		1.80	3.59
28	11.359	98.402	6	254		1.90	3.80
29	5.426	163.949	66	254		1.31	2.63
30	4.361	179.686	92	254		1.18	2.36

Determination of the size of Nanoparticles using ImageJ software.

- Palladium-gold nanoparticles (desalted) (Figure 15)

	Area	Mean	Min	Max		radius (nm)	diameter (nm)
1	5.785	15.938	0	255		1.48	2.96
2	6.87	31.156	0	255		1.48	2.96
3	6.87	75.733	0	255		0.84	1.68
4	2.221	40.029	0	255		1.18	2.36
5	4.39	12	0	255		1.20	2.40
6	4.507	81.103	0	255		0.94	1.88
7	2.763	71.495	0	255		1.36	2.71
8	5.772	17.685	0	255		1.28	2.56
9	5.165	23.588	0	255		1.62	3.24
10	8.239	99.922	0	255		1.20	2.40
11	4.507	0.731	0	255		0.94	1.88
12	2.763	58.388	0	255		1.28	2.56
13	5.165	49.088	0	255		0.94	1.88
14	2.763	91.752	0	255		1.03	2.05
15	3.306	35.859	0	255		1.01	2.02
16	3.19	46.457	0	255		0.94	1.88
17	2.763	121.542	0	255		0.91	1.81
18	2.583	73.95	0	255		0.84	1.68
19	2.221	115.64	0	255		0.91	1.81
20	2.583	150.45	0	255		0.84	1.68
21	2.221	90.436	0	255		1.01	2.02
22	3.19	47.49	0	255		1.11	2.23
23	3.9	126.656	0	255		1.03	2.05
24	3.306	131.484	0	255		0.85	1.71
25	2.286	122.458	0	255		0.85	1.71
26	2.286	106.61	0	255		1.28	2.56
27	5.165	18.488	0	255		1.28	2.56

Determination of the size of Nanoparticles using ImageJ software.

- Palladium (desalted and purified) (Figure 17)

	Area	Mean	Min	Max		radius (nm)	diameter (nm)
1	8.947	23.721	0	255		1.69	3.38
2	9.987	0	0	0		1.78	3.57
3	3.329	55.781	0	255		1.03	2.06
4	5.41	0	0	0		1.31	2.62
5	9.987	26.562	0	255		1.78	3.57
6	6.658	63.75	0	255		1.46	2.91
7	4.577	63.75	0	255		1.21	2.41
8	6.242	80.75	0	255		1.41	2.82
9	8.322	25.5	0	255		1.63	3.26
10	7.282	0	0	0		1.52	3.04
11	14.148	37.5	0	255		2.12	4.24
12	8.947	5.93	0	255		1.69	3.38
13	3.537	15	0	255		1.06	2.12
14	5.41	4.904	0	255		1.31	2.62
15	4.577	0	0	0		1.21	2.41
16	6.658	19.922	0	255		1.46	2.91
17	8.218	6.456	0	255		1.62	3.23
18	7.282	65.571	0	255		1.52	3.04
19	17.061	13.994	0	255		2.33	4.66
20	3.849	0	0	0		1.11	2.21
21	4.369	24.286	0	255		1.18	2.36
22	6.346	29.262	0	255		1.42	2.84
23	13.836	28.759	0	255		2.10	4.20
24	15.397	5.169	0	255		2.21	4.43
25	13.108	16.19	0	255		2.04	4.09
26	5.306	25	0	255		1.30	2.60
27	5.41	19.615	0	255		1.31	2.62
28	15.709	10.132	0	255		2.24	4.47
29	5.306	50	0	255		1.30	2.60
30	6.242	59.5	0	255		1.41	2.82
31	7.49	24.792	0	255		1.54	3.09
32	4.369	18.214	0	255		1.18	2.36
33	4.369	36.429	0	255		1.18	2.36
34	4.577	17.386	0	255		1.21	2.41
35	13.836	26.842	0	255		2.10	4.20
36	7.49	24.792	0	255		1.54	3.09

- Palladium with HAADF (desalted and purified) (Figure 18)

	Area	Mean	Min	Max		radius (nm)	diameter (nm)
1	4.967	84.618	71	93		1.26	2.51
2	2.17	86.413	84	100		0.83	1.66
3	2.129	86.353	78	101		0.82	1.65
4	6.574	85.676	81	100		1.45	2.89
5	3.047	85.863	85	100		0.98	1.97
6	12.041	84.461	64	93		1.96	3.92
7	4.32	84.966	76	95		1.17	2.35
8	7.638	85.014	68	100		1.56	3.12
9	20.535	83.984	60	88		2.56	5.11
10	8.306	85.98	83	101		1.63	3.25
11	7.283	85.358	81	97		1.52	3.05
12	3.673	85.562	77	98		1.08	2.16
13	3.694	85.492	84	99		1.08	2.17
14	3.694	85.09	85	92		1.08	2.17
15	5.009	85.479	85	101		1.26	2.53
16	2.63	85.484	85	96		0.91	1.83
17	4.341	86.524	81	103		1.18	2.35
18	11.165	84.794	66	100		1.89	3.77
19	1.461	86.843	85	97		0.68	1.36
20	6.49	85.35	70	100		1.44	2.87
21	3.089	85.696	85	100		0.99	1.98
22	10.205	85.147	80	100		1.80	3.60
23	9.099	84.908	71	95		1.70	3.40
24	2.838	86.809	76	101		0.95	1.90
25	3.151	86.675	85	101		1.00	2.00
26	3.673	86.165	85	103		1.08	2.16
27	9.412	85.357	81	97		1.73	3.46
28	5.176	85.024	85	91		1.28	2.57
29	1.649	87.392	85	100		0.72	1.45

- Palladium-gold nanoparticles (desalted and purified) (Figure 18)

	Area	Mean	Min	Max		radius (nm)	diameter (nm)
1	5.377	215.222	102	254		1.31	2.62
2	3.132	194.518	123	254		1.00	2.00
3	3.132	202.215	117	254		1.00	2.00
4	4.426	234.415	128	254		1.19	2.37
5	5.072	199.14	92	254		1.27	2.54
6	3.83	220.702	125	254		1.10	2.21
7	2.181	179.424	88	254		0.83	1.67
8	1.42	195.259	93	254		0.67	1.34
9	2.536	178.97	85	254		0.90	1.80
10	2.181	133.227	65	234		0.83	1.67
11	3.83	136.57	61	254		1.10	2.21
12	1.775	148.621	78	242		0.75	1.50
13	4.312	214.103	89	254		1.17	2.34
14	3.83	196.96	74	254		1.10	2.21
15	3.246	185.254	94	254		1.02	2.03
16	2.714	183.318	75	254		0.93	1.86
17	2.714	140.533	62	237		0.93	1.86
18	4.844	160.293	67	254		1.24	2.48
19	4.426	170.249	76	254		1.19	2.37
20	2.714	139.355	53	254		0.93	1.86
21	4.312	178.797	68	254		1.17	2.34
22	4.426	204.074	100	254		1.19	2.37
23	2.714	183.355	73	254		0.93	1.86
24	3.83	163.834	70	254		1.10	2.21
25	2.245	198.277	99	254		0.85	1.69
26	3.246	163.867	64	254		1.02	2.03
27	4.312	121.571	26	254		1.17	2.34
28	4.844	174.5	65	254		1.24	2.48
29	2.181	202.302	101	254		0.83	1.67
30	5.668	207.911	119	254		1.34	2.69
31	4.312	211.297	99	254		1.17	2.34
32	2.714	216.248	92	254		0.93	1.86
33	2.714	147.472	53	254		0.93	1.86